

T. Mart and N. Nurhadiansyah

Are hyperon resonances required in the elementary $K^+\Lambda$ photoproduction?*

Received: date / Accepted: date

Abstract We have investigated the role of hyperon resonances in the kaon photoproduction process, $\gamma p \rightarrow K^+\Lambda$, by using a covariant isobar model. To this end, new experimental data are used in the fitting process, whereas the old SAPHIR 1998 data are also used for comparison. The result indicates that the $\Lambda(1600)P_{01}$ and $\Lambda(1810)P_{01}$ hyperon resonances can significantly reduce the χ^2 and, simultaneously, can increase the hadronic form factor cut-off in the background terms. This finding is different from the result of the previous studies, which showed that the $\Lambda(1800)S_{01}$ was important for this purpose, instead of the $\Lambda(1600)P_{01}$.

Keywords Kaon photoproduction · Hyperon resonance · Isobar model

1 Introduction

Recently, it has been shown that kaon photoproduction process provides an important tool for investigating missing resonances, the resonances predicted by constituent quark models but not observed yet by the Particle Data Group (PDG) [1]. The relatively small decay widths to pion-nucleon channel are believed to be the reason behind this fact. However, certain constituent quark models [2, 3] predict that these resonances have larger decay widths to other channels, such as kaon-hyperon ones. Thus, kaon photoproduction is well suited to shed more light on the existence of these missing resonances.

Whereas nucleon resonances have been intensively investigated by using kaon photoproduction, there has been no thorough study on hyperon resonances by means of this process. Ideally, such a study should be performed by using the kaon-nucleon scattering, in which hyperon resonances propagate in the s -channel. Furthermore, kaon-nucleon scattering experiment has become the main focus of recent experimental activities at JPARC in Japan [4]. Nevertheless, in order to achieve an accuracy similar to that obtained in experiments using electromagnetic beams performed at Jefferson Lab, MAMI, and Spring8, one needs very intense kaon beam. Moreover, it is widely understood that hadronic interaction is not as "clean" as the electromagnetic one. In view of this, kaon photoproduction could offer a complementary solution, since the hyperon resonance propagates in the u -channel and, therefore, the process is sensitive to certain observables at backward kaon scattering angles.

More than a decade ago it was found that the second peak in the cross section of SAPHIR data [5] can be nicely reproduced by including a missing $D_{13}(1895)$ nucleon resonance in a covariant isobar model. [6]. An isobar model which includes this resonance and hadronic form factors was fitted to the SAPHIR data. The form factor cut-off Λ was allowed to vary during the fitting process and it was found that $\Lambda = 0.64$ GeV. Although there is no tool to measure this form factor directly, since it is an off-shell form factor, such a small cut-off was considered to be unreasonably soft [7] and the form factors were considered as an artificial

* Dedicated to Professor Henryk Witala at the occasion of his 60th birthday.

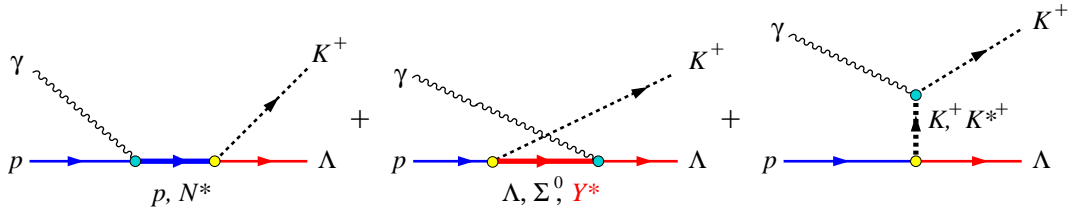


Fig. 1 Feynman diagrams for $K^+\Lambda$ photoproduction on the proton. The hyperon resonance Y^* contributes to the u -channel process (middle diagram).

mechanism required just to suppress the diverging Born terms at high energies. Instead of using this resonance and an artificial cut-off, Ref. [7] proposed to use $\Lambda(1800)S_{01}$ and $\Lambda(1810)P_{01}$, which were claimed to have the same ability to suppress the Born terms, while simultaneously to keep the form factor sufficiently “hard”.

Since the number of experimental data at present is almost one order of magnitude larger than the number when the claim was proposed, we believe that it is timely to check whether or not the $\Lambda(1800)S_{01}$ and $\Lambda(1810)P_{01}$ hyperon resonances are still able to help the model in improving the agreement with experimental data, while keeping the hadronic cut-off reasonably “hard”. It is the main purpose of the present paper to discuss the limitation of the claim. Furthermore, it is also important to investigate the role of other hyperon resonances in kaon photoproduction. Since at present the number of data becomes sufficiently large, while the corresponding error bars are considerably small, we believe that there are just few degrees of freedom left in the model. This is obviously in contrast to the former situation.

In Section 2 we briefly review the isobar model used in our investigation. Section 3 discusses the numerical results of our investigation. We will summarize our discussion and conclude our findings in Section 4.

2 Isobar Model

The elementary process for $K^+\Lambda$ photoproduction on the proton target can be written as

$$\gamma(k) + p(p_p) \rightarrow K^+(q) + \Lambda(p_\Lambda) . \quad (1)$$

Theoretically, this process can be described by utilizing an isobar model. At a tree-level approximation, the process is schematically shown in Fig. 1. The elementary transition operator can be calculated from the appropriate Feynman diagrams in Fig. 1 and decomposed into

$$\mathcal{M}_{\text{fi}} = \bar{u}(\mathbf{p}_\Lambda) \sum_{i=1}^4 A_i(s, t, u) M_i u(\mathbf{p}_p) . \quad (2)$$

where s, t and u are the Mandelstam variables. The gauge and Lorentz invariant matrices M_i can be found, e.g., in Ref. [8]. All relevant observables required in this investigation can be calculated from the functions $A_i(s, t, u)$ (see, e.g. Ref. [9]).

The background terms of the model consist of the standard s -, t -, and u -channel Born terms and appropriate kaon and hyperon resonances in the t - and u -channel, as shown in Fig. 1. A long standing problem in the isobar model is the inclusion of nucleon, kaon, and hyperon resonances. The number of resonances available from the PDG listing [1] was considered as too large. In the past, the number of experimental data was very limited. Using a few well known resonances one could explain all available data. In fact, the main topic of discussions in the past is how to constrain the number of resonances in the phenomenological models. However, the situation seems to change with the coming of precise experimental data from recent measurements in modern laboratories. These data include not only differential cross sections, but also single and double polarization observables that are very sensitive to the choice of resonances in the model. Thus, the new data could provide a stringent constraint to the existing phenomenological models. In fact, the new data can shed more light on the existence of the missing resonances.

In this study we include all nucleon resonances in the PDG listing [1] that have masses between the $K^+\Lambda$ threshold (1.609 GeV) and 2.2 GeV. The resonance spin is limited only up to 3/2 in order to simplify the formalism. In addition, we also include the $P_{11}(1840)$ state, which was found in Ref. [10] to have important contribution in the photoproduction of $K^+\Lambda$, $K^+\Sigma^0$, and $K^0\Sigma^+$. Our recent study [11] corroborates this

finding. In the t -channel, we use two vector mesons with different parities, i.e. the $K^*(892)$ and $K_1(1270)$, that have been shown to provide a significant suppression to the divergence of the Born terms. As a starting point, we include two hyperon resonances in the u -channel, which were claimed by Ref. [7] to provide also significant suppression, so that the hadronic form factor cut-off can be constrained to a reasonable value. Furthermore, to account for hadronic structure in the hadronic vertices we include hadronic form factors in a gauge invariant fashion [12]. For this purpose, we choose the dipole-type,

$$F(q^2) = \frac{\Lambda_{\text{had}}^4}{\Lambda_{\text{had}}^4 + (q^2 - m^2)^2}, \quad (3)$$

where Λ_{had} is the cut-off parameter, q^2 is the squared of four-momentum of the off-shell intermediate particle with the corresponding mass m . Note that this form has been used in most analyses of the meson-nucleon scattering as well as meson photoproduction. Clearly, the use of other types of form factor is also possible in this case and the effect of different hadronic form factors on the isobar model could become an important issue in kaon photoproduction [13].

3 Numerical Result

3.1 Reanalyzing the Old Models

As a first step, we try to reproduce the claim in Ref. [7], i.e. certain hyperon resonances can help to suppress the diverging Born terms. To this end we fit a model consisting of the Born terms, $K^*(892)$, $K_1(1270)$, $N(1650)S_{11}$, $N(1710)P_{11}$, and $N(1720)P_{13}$ resonances. For the sake of brevity we call this Born and resonance configuration as the standard configuration. Using this standard configuration we fit the model to the SAPHIR [5] and new data and call the result as Model A and B, respectively. In the next step we add the missing $D_{13}(1895)$ nucleon resonance [6] into the two models and repeat the fitting process. Having finished this step we continue to include the $\Lambda(1800)S_{01}$, $\Lambda(1810)P_{01}$ in the standard configuration and repeat the fitting process. Finally, we include the $D_{13}(1895)$, $\Lambda(1800)S_{01}$, and $\Lambda(1810)P_{01}$ in the model and fit to the SAPHIR and new data as before. The complete result obtained from this procedure is given in Table 1 in terms of the obtained χ^2/N , where N indicates the number of degrees of freedom, i.e. $N = N_{\text{data}} - N_{\text{parameter}}$. We also quote the result of Ref. [7] in Table 1 for comparison. Note that in order to maintain consistency with the claim of Ref. [7], in all configurations we limit the hadronic form factor cut-off to be $\Lambda \geq 1.6$ GeV during the fitting process.

Table 1 Comparison between χ^2/N obtained by different number and configuration of resonances. Model A has the same resonance configuration as in Ref. [7] and fitted to the same (SAPHIR) data. Model B uses the same configuration but fitted to the new data.

Configuration	Ref. [7]	Model A	Model B
Standard	10.32	8.11	14.05
Standard + $N(1895)D_{13}$	7.38	4.11	6.12
Standard + $\Lambda(1800)S_{01}$, $\Lambda(1810)P_{01}$	3.43	4.77	9.18
Standard + $N(1895)D_{13}$, $\Lambda(1800)S_{01}$, $\Lambda(1810)P_{01}$	2.65	2.68	4.07

It is obvious that our present calculation is in fair agreement with the result of Ref. [7]. The difference in the χ^2/N might originate from the error-bars used in the fitting process. In our calculation, we have also included systematic error-bars in addition to statistical ones. This is reflected by the fact that the obtained χ^2/N in Model A is mostly smaller than those in Ref. [7]. Nevertheless, Model A reveals an interesting fact, i.e. the use of the $D_{13}(1895)$ resonance to suppress the diverging Born terms is more effective than the use of two hyperon resonances, the $\Lambda(1800)S_{01}$ and $\Lambda(1810)P_{01}$, as suggested by Ref. [7]. Indeed, this phenomenon also appears when we use the new experimental data (with more than 3500 data points) as shown by Model B in the fourth column of Table 1.

By comparing the results of Model A and B in the third and fourth columns of Table 1, respectively, it is apparent that the resonance configuration suggested by Table 1 is unable to produce a reasonable agreement

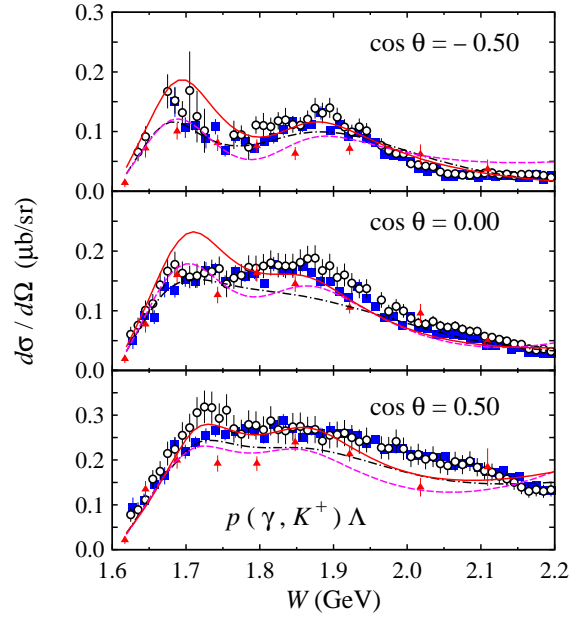


Fig. 2 Comparison between differential cross sections obtained from Model A (dashed lines), Model B (solid lines), and Kaon-Maid (dash-dotted lines). Experimental data are from the CLAS collaboration (solid squares [14] and open circles [15]) and SAPHIR collaboration (solid triangles) [5].

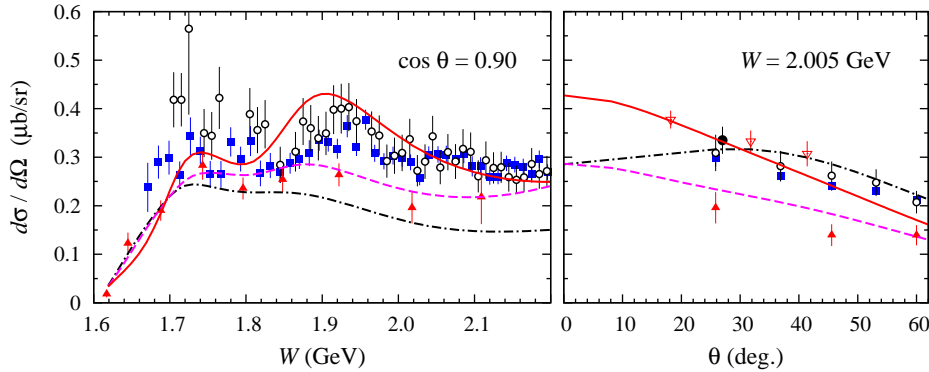


Fig. 3 Same as Fig 2, but for the forward angles, where experimental data are still available for comparison. The behavior of the models at very forward angles can be seen in the right panel. Here, open triangle indicates the LEPS data [16], while solid circle comes from an old experiment [17].

with experimental data. Furthermore, we can also clearly see that including the missing $D_{13}(1895)$ nucleon resonance as suggested in Ref. [6] results in a significant reduction of χ^2/N . Nevertheless, combining this resonance with $\Lambda(1800)S_{01}$ and $\Lambda(1810)P_{01}$ in the standard configuration will reduce the χ^2/N to 4.07, which is still beyond a reasonable value for a good agreement between model calculation and experimental data. The reason for that is obviously displayed in Fig. 2, where we compare the calculated differential cross sections obtained from Model A and B with the prediction of Kaon-Maid [18]. Presumably, more nucleon resonances are required to explain the structures, which cannot be reproduced by both Model A and B. This topic will be discussed in the next subsection, when we include the higher nucleon resonances, which are found to be important in the coupled-channels study [10]. We note that the higher nucleon resonances have been also found to play an important role in the $K^*\Lambda$ photoproduction [19].

At this stage, it is also important to revisit the problem of kaon photoproduction at forward angles. As discussed in Ref. [20], the use of hadronic form factor in Kaon-Maid [18] has led to an underprediction of differential cross section data at forward angles. Near forward angles, where experimental data are still available,

Table 2 Nucleon and hyperon resonances used in the present investigation along with their properties. Most of the data are taken from Particle Data Group (PDG) listings [1]. Otherwise, the values originates from our previous calculation [11].

Resonance		Mass	Width
Short Symbol	PDG Symbol	(MeV)	(MeV)
$S_{11}(1650)$	$N(1650)S_{11}$	1650	150
$S_{11}(2090)$	$N(2090)S_{11}$	2090	400
$P_{11}(1710)$	$N(1710)P_{11}$	1710	100
$P_{11}(1880)$	$N(1880)P_{11}$	1952	413
$P_{11}(2100)$	$N(2100)P_{11}$	2100	113
$P_{13}(1720)$	$N(1720)P_{13}$	1720	150
$P_{13}(1900)$	$N(1900)P_{13}$	1900	498
$D_{13}(1700)$	$N(1700)D_{13}$	1700	100
$D_{13}(2080)$	$N(2080)D_{13}$	2080	450
$\Lambda^*(1405)$	$\Lambda(1405)S_{01}$	1406	50
$\Lambda^*(1600)$	$\Lambda(1600)P_{01}$	1600	150
$\Lambda^*(1670)$	$\Lambda(1670)S_{01}$	1670	35
$\Lambda^*(1800)$	$\Lambda(1800)S_{01}$	1800	300
$\Lambda^*(1810)$	$\Lambda(1810)P_{01}$	1810	150
$\Sigma^*(1660)$	$\Sigma(1660)P_{11}$	1660	100
$\Sigma^*(1750)$	$\Sigma(1750)S_{11}$	1750	90

the situation is depicted in Fig. 3. The problem is apparent in the case of Kaon-Maid, which originates from the extracted form factor cut-off. We notice that the background terms of Kaon-Maid is strongly suppressed by a very soft form factor, i.e. the dipole form factor given by Eq. (3) with $\Lambda_{\text{had}} = 0.64$ GeV.

However, in the case of Model A and B we obtain the relatively larger cut-offs. i.e. $\Lambda_{\text{had}} = 1.90$ GeV and 1.60 GeV, respectively, which correspond to relatively harder form factors. Thus, both models do not exhibit a problem at forward angles as in the case of Kaon-Maid, although we also notice that Model A cannot reproduce experimental data at this kinematics, since it was fitted to old SAPHIR data [5]. Nevertheless, from the right panel of Fig. 3 we can see that the hard hadronic form factors in both models are represented by the increase of the cross section as the kaon angle θ approaches forward directions.

We conclude this subsection by emphasizing that to suppress the diverging Born terms the use of the $\Lambda(1800)S_{01}$ and $\Lambda(1810)P_{01}$ hyperon resonances as suggested by Ref. [7] is less effective than the use of the missing $D_{13}(1895)$ nucleon resonance as proposed in Ref. [6]. However, it is true that the soft hadronic cut-off leads to a strong suppression of the cross section at forward directions.

3.2 Adding More Nucleon Resonances

From the discussion in the previous subsection it is obvious that the number of resonances must be increased for the purpose of explaining other structures appearing in the new data and, therefore, minimizing the χ^2 . Using the modified standard configuration we obtained the best $\chi^2/N = 4.07$ (see Model B, the fourth column of Table 1), which indicates a rather poor agreement between model calculation and experimental data. To this end, we will use the nucleon resonance configuration in the isobar model developed in our recent study [11], which is able to nicely reproduce the presently available data. The model is constructed by using the same standard configuration (see Table 1) and, in addition, the $P_{13}(1720)$, $P_{11}(1840)$, $P_{13}(1900)$, $D_{13}(2080)$, $S_{11}(2090)$, as well as $P_{11}(2100)$ resonances. Note that these resonances have been found to be important in photoproduction of $K^+\Lambda$, $K^+\Sigma^0$, and $K^0\Sigma^+$ [10]. In the original model [11], the $\Lambda^*(1800)$ and $\Lambda^*(1810)$ hyperon resonances have been also included in order to achieve the best agreement with experimental data. In this study we start our fitting process by including all available Λ^* and Σ^* in the PDG listing [1] with spin 1/2. We do not include higher spin hyperon resonances for the sake of simplicity. Table 2 summarizes the nucleon and hyperon resonances used in the present study.

Having finished the fitting process we start excluding each of the hyperons and repeat the process in order to estimate the role of each hyperon in minimizing the χ^2/N and, at the same time, keeping the hadronic form

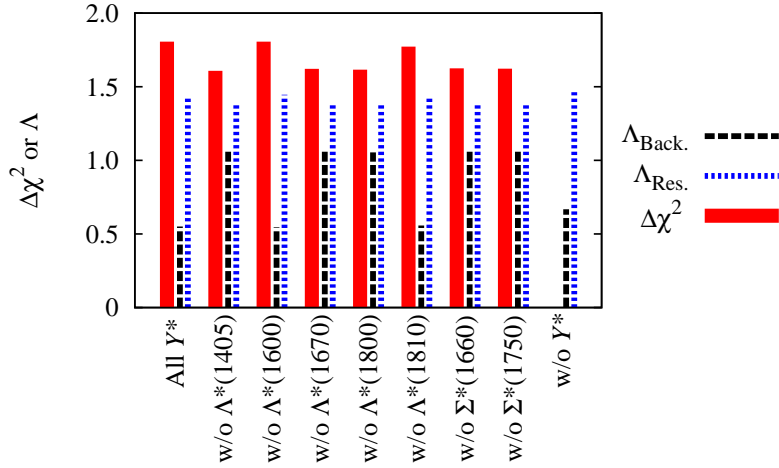


Fig. 4 Contribution of the hyperon resonance(s) in reducing the χ^2 compared with the extracted background and resonance hadronic form factor cut-offs. Shown in this figure are results from different fits obtained with all resonances, without (w/o) specific resonance, and without all hyperon resonances included in the model.

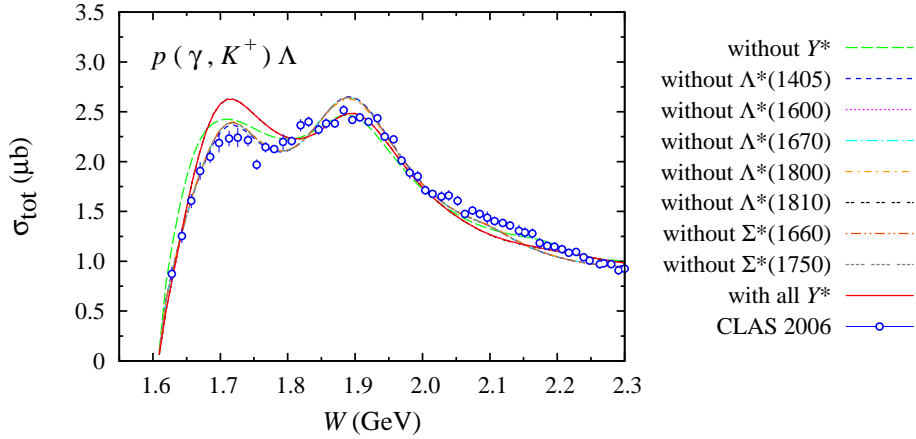


Fig. 5 Total cross section of the $K^+\Lambda$ photoproduction obtained from a number of model calculations. Notation of the curves are given on the right hand side of the figure. Experimental data are from the CLAS collaboration [14]. These data were not used in the fitting process of the present investigation.

factor cut-off always reasonably hard. The result is shown in Fig. 4, where we have defined

$$\Delta\chi^2 = \frac{|\chi_{\text{excl.}}^2 - \chi_{\text{no}}^2|}{1000}, \quad (4)$$

with $\chi_{\text{excl.}}^2$ indicates the χ^2 obtained with one particular hyperon excluded from the model, whereas χ_{no}^2 is the χ^2 obtained without including the hyperon resonance at all. The factor of 1000 in the denominator is used in order to fit the result on the scale. Thus, the $\Delta\chi^2$ in Eq. (4) measures the role of one particular hyperon resonance in reducing the χ^2 , i.e. the larger the value of $\Delta\chi^2$, the more important is the resonance.

From Fig. 4 we can clearly see that only two hyperon resonances can significantly reduce the χ^2 , i.e. the $\Lambda^*(1600)$ and $\Lambda^*(1810)$. The latter has been found as an important hyperon resonance in kaon photoproduction since more than a decade ago, but the former is new. Interestingly, excluding these resonances from the model leads to very soft background cut-offs, which is clearly exhibited by the shorter dashed (black) lines in Fig. 4. Therefore, both hyperon resonances are important to reduce the χ^2 as well as to keep the hadronic cut-off reasonably hard.

It is also important to note that in the resonance sector there is no need to suppress the amplitude, since the resonances do not produce a diverging amplitude, in spite of the fact that the covariant Feynman diagrams also

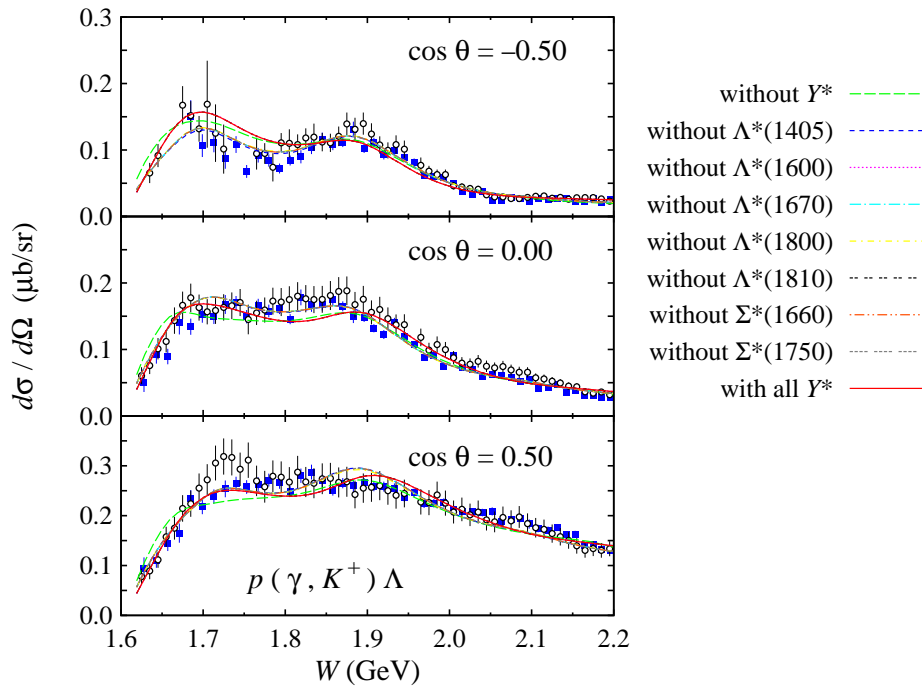


Fig. 6 Same as Fig 5, but for differential cross section. Experimental data are taken from the CLAS collaboration (solid squares [14] and open circles [15]).

create additional background amplitudes. Furthermore, Fig. 4 implies that including all hyperon resonances in the model were not recommended, since the background cut-off would significantly drop to a very soft value. This indicates that the χ^2 alone cannot be used as the only measure for a good agreement with experimental data. The soft hadronic form factor would be also obtained if we did not include any hyperon resonance. To conclude this result, we may say that Fig. 4 reveals the dual-role of hyperon resonances, i.e. reducing the χ^2 value and, simultaneously, keeping the hadronic cut-off to a reasonably hard value.

Comparison between experimental data and model calculations with or without (a specific or all) hyperon resonances are displayed in Fig. 5. Here we can see that the model obtained by including all hyperon resonances and that obtained by excluding the $\Lambda^*(1600)$ or $\Lambda^*(1810)$ hyperon resonance fail to reproduce the first peak of the total cross section. Since a number of curves in this figure is coincidence with each other, we have checked the numerical results and confirmed this finding. Again, this indicates that we cannot neglect these hyperon resonances in $K^+\Lambda$ photoproduction.

For the second peak in the total cross section we see that the predictions of these three models seem to overpredict the data. However, we observe that this happens because at this point the new version of CLAS differential cross section data [15] are substantially larger than the previous version [14]. This could be the origin of the problem. The comparison in this case is given in Fig. 6 for the differential cross section.

The more obvious difference between model calculations is observed in the forward region, as depicted in Fig. 7. From the left panel of Fig. 7 we might conclude that the problem in the fitting process is due to the scattered experimental data. However, the right panel of Fig. 7 displays the important message: using the soft hadronic form factor obtained in a model with all hyperon resonances included, a model without $\Lambda^*(1600)$, or a model without $\Lambda^*(1810)$, as shown in Fig. 4, results in a suppressed differential cross section at very forward angles. Therefore, the result of our present study provides a more solid evidence of the origin of this suppression, which was predicted previously in Ref. [20].

It has been also widely known that both single- and double-polarization observables are sensitive to the choice of resonances in the model. Therefore, in Figs. 8 and 9 we display the result of our present investigation in the case of recoiled hyperon polarization P and beam-recoil double polarizations C_x and C_z , respectively. However, we observe that the recoil polarization does not show a remarkable sensitivity, except at $W \leq 1.7$

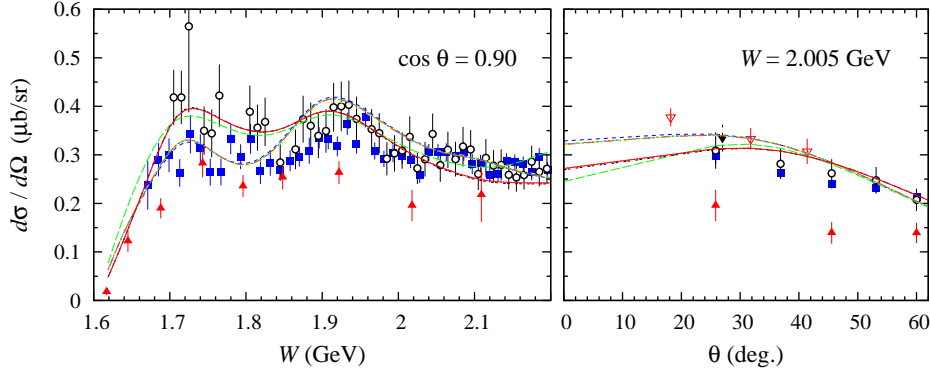


Fig. 7 Differential cross sections in the forward region as in Fig. 3, but for different fits using different hyperon resonances. Notation of the curves is as in Fig. 5.

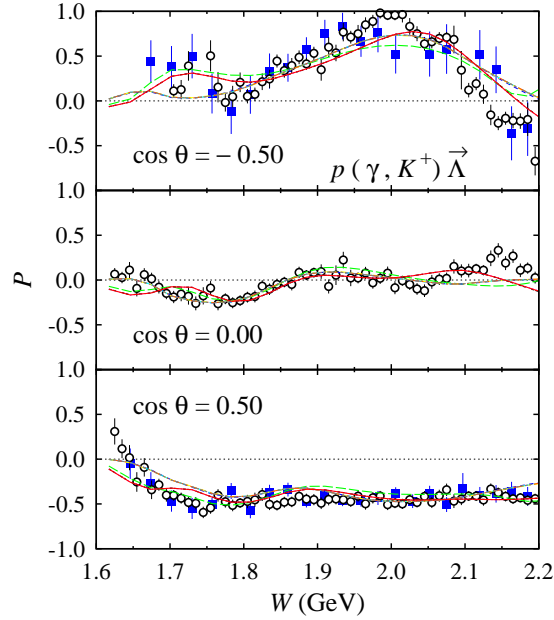


Fig. 8 Comparison between model calculations and experimental data for the recoil polarization observable P . Experimental data are taken from the CLAS collaboration (solid squares [14] and open circles [15]). Notation of the curves is as in Fig. 5.

GeV. In this kinematics we find sizable differences between models, but within the present error bars they are still difficult to distinguish.

The beam-recoil double polarization C_x shown in Fig. 9 is found as the most sensitive observable for our present purpose, especially at backward directions. In Fig. 9 it is shown that excluding the $\Lambda^*(1600)$ and $\Lambda^*(1810)$ resonances results in a clear disagreement between data and model calculations. We notice that the difference decreases in the forward region. In the case of double polarization C_x the situation is difficult, due to the deficiency of the model, except at a very forward angle. Unfortunately, in this kinematics the difference between model calculations is smaller than that obtained in other kinematics. Thus, this observable is not recommended for the present purpose.

Our present finding is therefore partly different from the result of the previous work [7], i.e. instead of the $\Lambda(1800)S_{01}$ resonance we found the $\Lambda(1600)P_{01}$ resonance to be the important one. This difference presumably originates from the new data used in the present study.

From the propagator behavior it could be expected that the u -channel resonances would have dominant effects in the backward directions, in Fig. 10 we display our result for this kinematics. Obviously the effect of using different hyperon resonances is apparent here. By comparing Figs. 7 and 10 we can see that the effect

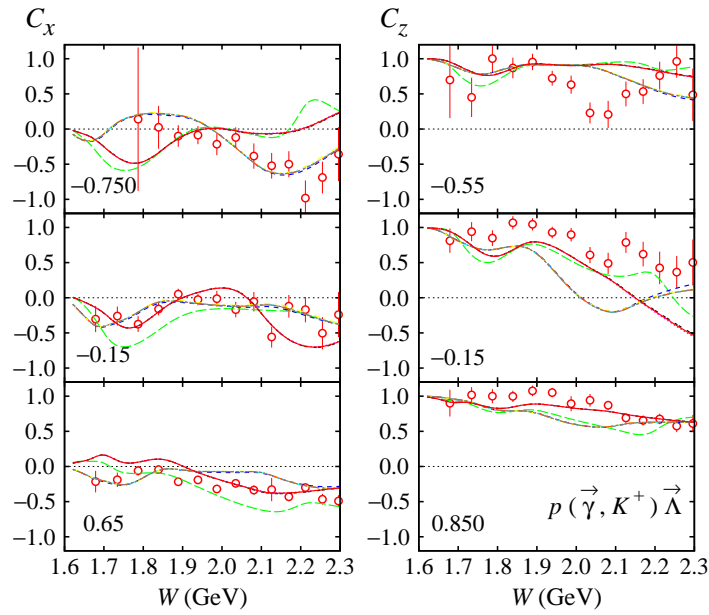


Fig. 9 The beam-recoil double polarization observables C_x (left panel) and C_z (right panel). Experimental data are from the CLAS collaboration [21]. Notation of the curves is as in Fig. 5.

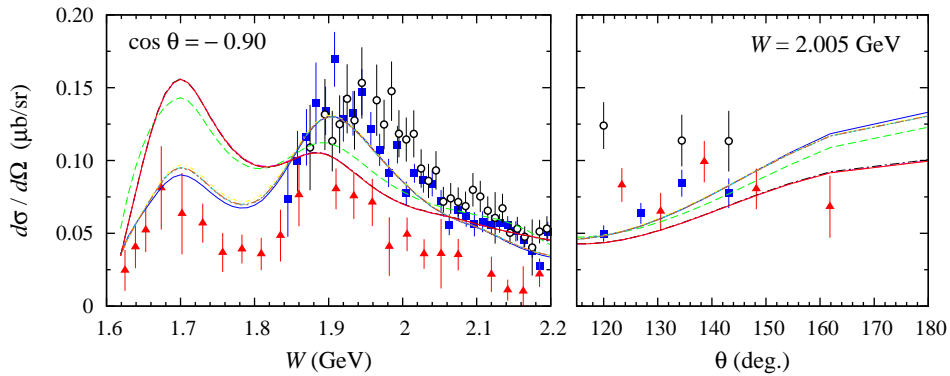


Fig. 10 Differential cross sections as in Fig. 7, but for the backward directions.

found in the forward region is even amplified in the backward direction. The left panel of Fig. 10 clearly confirms that the effect is largest at kaon angle 180° . Unfortunately, experimental data at this kinematics cannot resolve this effect.

3.3 Sensitivity of the Result to the Hadronic Form Factor Cut-Off

How sensitive our result to the variation of the hadronic form factor cut-off would be also an interesting question to address. To investigate this sensitivity we make use of the isobar model proposed in Ref. [11], where the $\Lambda(1800)S_{01}$ and $\Lambda(1810)P_{01}$ hyperon resonances have been already included. However, to account for the result obtained in the previous section, in the present discussion we add the $\Lambda(1600)P_{01}$ hyperon resonance to the model and refit the model predictions to experimental data. The χ^2/N reduces from 2.57 to 2.49. The hadronic form factor cut-offs for the background and resonance terms are obtained to be 1.055 and 1.385 GeV, respectively. Thus, we believe that the model is sufficiently good for our present purpose. Using this model we vary the background cut-off from 0.5 to 2 GeV with 0.05 GeV step, refit the experimental data, and calculate the χ^2/N . The result is depicted in Fig. 11 by the solid line. For comparison, we also propose a model without hyperon resonance, for which the obtained hadronic cut-off is 0.769 GeV and the best χ^2/N

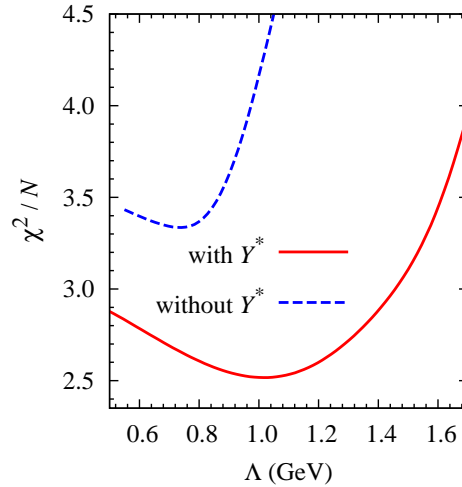


Fig. 11 Comparison between the χ^2/N obtained from a model including hyperon resonances (solid line) and that excluding hyperon resonances (dashed line) plotted as a function of the hadronic form factor cut-off of the Born terms.

is 3.34. The corresponding variation of χ^2/N as a function of the background cut-off is shown in Fig. 11 by using the dashed line.

It is obvious that the three hyperon resonances are able to significantly improve the agreement with experimental data and shift the desired cut-off to a larger value. Although the two cases are clearly different, both share the same behavior, i.e. increasing the cut-off value would directly increase the disagreement between model calculations and experimental data. Especially, in the case of the model without hyperon resonance, where the χ^2/N increases dramatically with slightly increasing the cut-off. The result indicates that in these models obtaining a softer hadronic form factor would be much easier than a harder one. Put in other words, the models are less sensitive to the variation of the cut-off in the smaller cut-off region, but very sensitive in the larger one.

4 Summary and Conclusion

We have investigated the role of hyperon resonances in the elementary photoproduction of $K^+\Lambda$ by using isobar models. To this end, we have reproduced the previous claim that the $\Lambda(1800)S_{01}$ and $\Lambda(1810)P_{01}$ could increase the hadronic form factor cut-off to a harder region, by using the SAPHIR 1998 data. Using the new data, we have shown that the resonance configuration used to reproduce the SAPHIR 1998 data is insufficient to achieve a reasonably good agreement between model calculations and data. To overcome this problem we have added more nucleon resonances in the model. The model is able to nicely reproduce the new data. By making use of this model we have investigated all spin 1/2 hyperon resonances listed by the PDG. It is found that the $\Lambda(1600)P_{01}$ and $\Lambda(1810)P_{01}$ resonances are required to reduce the χ^2 and, simultaneously, to keep the hadronic form factor reasonably hard. Excluding one of these (or both) resonances from the model results in a suppression of differential cross section at forward angles. Our finding is therefore partly different from the result of previous studies. Our result confirms that the effect of the hyperon resonances is largest in the backward direction. The obtained model is very sensitive to the variation of the hadronic cut-off for the background terms, especially if no hyperon resonance were included. The sensitivity of the model implies that obtaining a model with softer cut-off is much easier than that with harder one.

Acknowledgements TM acknowledges the supports from the University of Indonesia and the Competence Grant of the Indonesian Ministry of National Education are gratefully acknowledged.

References

1. Beringer, J. *et al.*: Review of particle physics. Phys. Rev. D **86**, 010001 (2012)

2. Isgur, N. and Karl, G.: Hyperfine interactions in negative parity baryons. *Phys. Lett. B* **72**, 109-113 (1977); Koniuk, R. and Isgur, N.: Baryon decays in a quark model with chromodynamics. *Phys. Rev. D* **21**, 1868-1886 (1980)
3. Capstick, S. and Roberts, W.: Quasi-two-body decays of nonstrange baryons. *Phys. Rev. D* **49**, 4570-4586 (1994)
4. Noumi, H. *et al.*: "Spectroscopic study of hyperon resonances below $\bar{K}N$ threshold via the (K^-, n) reaction on deuteron", proposal for the J-PARC 50 GeV Proton Synchrotron, submitted to the 8th PAC meeting, July 2009. Available via J-PARC homepage: <http://j-parc.jp>.
5. Tran, M. Q. *et al.*: Measurement of $\gamma p \rightarrow K^+ \Lambda$ and $\gamma p \rightarrow K^+ \Sigma^0$ at photon energies up to 2 GeV. *Phys. Lett. B* **445**, 20-26 (1998)
6. Mart T., Bennhold C.: Evidence for a missing nucleon resonance in kaon photoproduction. *Phys. Rev. C* **61**, 012201 (1999)
7. Janssen, S., Ryckebusch, J., Van Nespen, W., Debruyne, D. and Van Caueren, T. : The role of hyperon resonances in $p(\gamma, K^+) \Lambda$ processes. *Eur. Phys. J. A* **11**, 105-111 (2001)
8. Mart, T. and van der Ventel, B. I. S.: Photo- and electroproduction of the hypertriton on ${}^3\text{He}$. *Phys. Rev. C* **78**, 014004 (2008)
9. Knöchlein, G., Drechsel, D., and Tiator, L.: Photo- and electroproduction of eta mesons. *Z. Phys. A* **352**, 327-343 (1995)
10. Sarantsev, A. V., Nikonov, V. A., Anisovich, A. V., Klempt, E. and Thoma, U.: Decays of baryon resonances into ΛK^+ , $\Sigma^0 K^+$ and $\Sigma^+ K^0$. *Eur. Phys. J. A* **25**, 441-453 (2005)
11. Mart, T. and Kholili, M. J.: Origin of the second peak in the cross section of the $K^+ \Lambda$ photoproduction. *Phys. Rev. C* **86**, 022201(R) (2012)
12. Habertzettl, H., Bennhold, C., Mart, T. and Feuster, T.: Gauge-invariant tree-level photoproduction amplitudes with form factors. *Phys. Rev. C* **58**, R40-R44 (1998)
13. Mart, T. and Sari, A.K.: Role of the hadronic form factors in the $\gamma p \rightarrow K^+ \Lambda$ process. (in preparation)
14. Bradford, R. *et al.*: Differential cross sections for $\gamma + p \rightarrow K^+ + Y$ for Λ and Σ^0 hyperons. *Phys. Rev. C* **73**, 035202 (2006)
15. McCracken, M.E., *et al.*: Differential cross section and recoil polarization measurements for the $\gamma p \rightarrow K^+ \Lambda$ reaction using CLAS at Jefferson Lab. *Phys. Rev. C* **81**, 025201 (2010)
16. Sumihama, M. *et al.*: The $\gamma p \rightarrow K^+ \Lambda$ and $\gamma p \rightarrow K^+ \Sigma^0$ reactions at forward angles with photon energies from 1.5 to 2.4 GeV. *Phys. Rev. C* **73**, 035214 (2006)
17. Feller, P. *et al.*: Photoproduction of $K^+ \Lambda^0$ and $K^+ \Sigma^0$ from hydrogen at constant momentum transfer t between 1.05 and 2.2 GeV. *Nucl. Phys. B* **39**, 413-420 (1972)
18. Available at the Maid homepage <http://www.kph.uni-mainz.de/MAID/kaon/kaonmaid.html>. The published versions can be found in: Ref. [6]; Mart, T.: Role of $P_{13}(1720)$ in $K\Sigma$ photoproduction. *Phys. Rev. C* **62**, 038201 (2000); Bennhold, C., Habertzettl, H., and Mart, T.: A new resonance in $K^+ \Lambda$ electroproduction: the $D_{13}(1895)$ and its electromagnetic form factors. [arXiv:nucl-th/9909022](https://arxiv.org/abs/nucl-th/9909022)
19. Kim, S.-H., Nam, S.-i., Oh, Y., and Kim, H.-C.: Contribution of higher nucleon resonances to $K^* \Lambda$ photoproduction. *Phys. Rev. D* **84**, 114023 (2011)
20. Bydžovský, P. and Mart, T.: Analysis of the consistency of kaon photoproduction data with Λ in the final state. *Phys. Rev. C* **76**, 065202 (2007)
21. Bradford, R. *et al.*: First measurement of beam-recoil observables C_x and C_z in hyperon photoproduction. *Phys. Rev. C* **75**, 035205 (2007)